



ELSEVIER



Int. J. Electron. Commun. (AEÜ) ■■■ (■■■) ■■■-■■■



www.elsevier.de/aeue

1

3 Cross-layer design based on RC-LDPC codes in MIMO channels with 5 estimation errors

5 Yuling Zhang^{a, b, *}, Dongfeng Yuan^{a, c}, Cheng-Xiang Wang^d

^aSchool of Information Science and Engineering, Shandong University, Jinan, Shandong 250100, PR China

7 ^bSchool of Computer Science and Technology, Ludong University, Yantai, Shandong 264025, PR China

^cState Key Laboratory of Integrated Service Networks, Xidian University, Xi'an 710071, PR China

9 ^dJoint Research Institute of Signal and Image Processing, School of Engineering and Physical Sciences, Heriot-Watt University, Edinburgh
EH14 4AS, UK

11 Received 7 June 2006; accepted 29 August 2007

13 Abstract

15 In this paper, we propose a cross-layer design framework combining adaptive modulation and coding (AMC) with hybrid
17 automatic repeat request (HARQ) based on rate-compatible low-density parity-check codes (RC-LDPC) in multiple-input
19 multiple-output (MIMO) fading channels with estimation errors. First, we propose a new puncturing pattern for RC-LDPC
21 codes and demonstrate that the new puncturing pattern performs similar to the random puncturing but is easier to apply. Then,
we apply RC-LDPC codes with the new puncturing pattern to the cross-layer design combining AMC with ARQ over MIMO
fading channels and derive the expressions for the throughput of the system. The effect of channel estimation errors on the
system throughput is also investigated. Numerical results show that the joint design of AMC and ARQ based on RC-LDPC
codes can achieve considerable spectral efficiency gain.

© 2007 Published by Elsevier GmbH

23 **Keywords:** Rate-compatible LDPC codes; Adaptive modulation and coding (AMC); Automatic repeat request (ARQ); Cross-layer design;
25 Multiple-input multiple-output (MIMO) channel

27 1. Introduction

29 The explosive growth of wireless packet data applica-
31 tions such as wireless Internet, interactive mobile multime-
33 dia applications, and interactive gaming has driven an un-
35 precedented revolution in wireless networks. Various applica-
tions in wireless networks require different quality of
service (QoS). In order to achieve efficient utilization of
scarce radio resources with different QoS requirements, the

cross-layer design approach has drawn significant research
attention allowing information sharing between different
layers of wireless networks. In the literature, various cross-
layer design schemes have been proposed. In [1], adaptive
modulation and coding (AMC) at the physical layer and
automatic repeat request (ARQ) at the data link layer were
jointly designed in order to maximize network capacity
under constrained QoS requirements. However, perfect
channel state information (CSI) was assumed and only single
input single output (SISO) scenario was considered in
[1]. This observation motivates us to extend the cross-layer
design in SISO channels to multiple-input multiple-output
(MIMO) channels using space-time block codes (STBCs)
with channel estimation errors.

It is widely accepted that powerful error control codes
should be employed to guarantee the high reliability of

* Corresponding author. School of Information Science and Engineer-
ing, Shandong University, Jinan, Shandong 250100, PR China. Tel.:
+86 531 88362525; fax: +86 531 88565167.

E-mail addresses: zhangyuling@hotmail.com,
zhangyuling@sdu.edu.cn (Y. Zhang), dfyuan@sdu.edu.cn (D. Yuan),
Cheng-Xiang.Wang@hw.ac.uk (C.-X. Wang).

wireless communication systems. Due to the special structure that enables simple encoding and decoding, rate-compatible (RC) codes have been shown to be favorable in both AMC and hybrid ARQ (HARQ) schemes. A RC code consists of a low rate mother code and several higher rate codes achieved through compatible puncturing. Hence, the decoder for the lowest rate code is compatible with the ones for higher rate codes and therefore no additional complexity is needed. In most AMC or HARQ schemes, RC punctured convolutional codes (RCPC) [2] or RC punctured turbo codes (RCPT) [3] were employed as the forward error control codes. Recently, RC low-density parity-check (RC-LDPC) codes [4,5] have raised a lot of research interests, e.g., finding the optimal puncturing pattern [6] and applying RC-LDPC codes to HARQ [5]. To the best of the authors' knowledge, however, there has not been any report on the application of RC-LDPC codes to cross-layer design schemes. In this paper, we first propose a new puncturing pattern, which is easy to realize, for RC-LDPC codes. Then, we apply RC-LDPC codes to the cross-layer design scheme combining the AMC with HARQ in MIMO fading channels.

The rest of this paper is organized as follows. In Section 2, we present the system model of the cross-layer design combining the AMC and HARQ in MIMO fading channels using STBCs. How to calculate the effective signal-to-noise ratio (SNR) and channel estimations are explained in Section 3, while the principle of the cross-layer design is illustrated in Section 4. In Section 5, we introduce the construction of RC-LDPC codes. In Section 6, we apply RC-LDPC codes to AMC-ARQ systems over MIMO fading channels with STBCs and get numerical results through simulations. Finally, some conclusions are drawn in Section 7.

2. System model

The system model of an AMC-ARQ system based on RC-LDPC codes in MIMO channels using STBCs is shown in Fig. 1. Assuming that there are N_T transmit antennas and N_R receive antennas, then the diversity order is defined as $K \triangleq N_T N_R$. The MIMO fading channel can be expressed as a matrix $\mathbf{H} = [h_{ij}]_{i,j=1}^{N_R, N_T}$, where h_{ij} is the channel coefficient between the j th transmit antenna and the i th receive

antenna. Under the assumption of independent Rayleigh fading, the channel coefficients h_{ij} are modeled as independent and identically distributed (i.i.d.) complex circular Gaussian random variables with zero mean and unit variance. The received signal can be expressed as

$$\mathbf{Y} = \mathbf{H}\mathbf{X} + \mathbf{V}, \quad (1)$$

where \mathbf{Y} is a $N_R \times T$ matrix of received symbols with T representing the number of symbols per antenna, \mathbf{X} is a $N_T \times T$ matrix of transmitted symbols, and \mathbf{V} is a $N_R \times T$ noise matrix with elements modeled as i.i.d. complex circular Gaussian random variables having zero mean and unit variance.

At the physical layer, there are multiple modulation and coding schemes (MCSs) available. Coded symbols are transmitted on a frame-by-frame basis through MIMO fading channels after space-time block coding. The CSI is estimated at the receiver and then sent back through a feedback channel to the AMC controller, which chooses the appropriate MCS in the next transmission accordingly.

At the data link layer, the selective repeat ARQ protocol is adopted to control packet retransmissions. When an error is detected in a packet, a retransmission request is generated and sent back to the transmitter via a feedback channel. For simplicity, we assume that the feedback channel is error free and has zero delay.

The packet and frame structures used in this paper are similar to those as illustrated in [1]. The only difference is that no cyclic redundancy check (CRC) codes are used in our system. This is due to the fact that LDPC codes are employed here, whose strong error detection ability enables them to act as error detection codes as well. It follows that there is no need to use CRC and thereby the system overhead can be significantly reduced. The error detection ability of LDPC codes is beyond the scope of this paper. In this paper, we simply assume that the error detection capability provided by the LDPC codes is sufficient for our system.

3. Effective SNR and channel estimation

In our system model shown in Fig. 1, the STBC encoder maps $R \leq T$ complex modulated symbols into N_T orthogonal

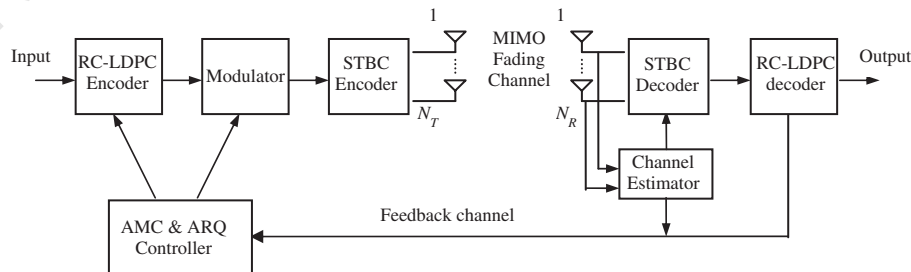


Fig. 1. System model.

1 complex symbol sequences of length T and then transmits
 2 them by N_T transmit antennas simultaneously. The coding
 3 rate of a STBC is therefore $R_c = R/T$. Let us define the
 4 average transmit power per stream/antenna as P_s . According
 5 to the effective SISO channel model for STBCs described in
 6 [7], the received symbol y before the maximum likelihood
 7 (ML) detection can be expressed as

$$y = \|\mathbf{H}\|_{\mathbb{F}}^2 s + v, \quad (2)$$

9 where s is the real or imaginary part of the transmitted com-
 10 plex symbol, v is the noise symbol with mean power σ^2 after
 11 STBC decoding, $\|\cdot\|_{\mathbb{F}}^2$ denotes the squared matrix Frobeni-
 12 us norm, and $\|\mathbf{H}\|_{\mathbb{F}}^2 = \sum_{i,j} h_{ij}^2$. At the receiver, the SNR
 13 is given by [8]

$$\gamma = \frac{P_s}{\sigma^2} \|\mathbf{H}\|_{\mathbb{F}}^2 = \frac{P_T}{\sigma^2 N_T R_c} \|\mathbf{H}\|_{\mathbb{F}}^2 = \frac{\bar{\gamma}}{N_T R_c} \|\mathbf{H}\|_{\mathbb{F}}^2, \quad (3)$$

15 where P_T is the total transmit power transmitted on N_T
 16 antennas per symbol duration and $\bar{\gamma} = P_T/\sigma^2$ is defined to
 17 be the average pseudo SNR. Since $\|\mathbf{H}\|_{\mathbb{F}}^2$ is the sum of $2K$
 18 i.i.d. χ^2 random variables, we can get the probability density
 19 function (PDF) of γ as follows [9]:

$$p_{\gamma}(\gamma) = \frac{\gamma^{K-1}}{\Gamma(K)} \left(\frac{N_T R_c}{\bar{\gamma}} \right)^K \exp\left(-\frac{N_T R_c}{\bar{\gamma}} \gamma\right), \quad \gamma \geq 0, \quad (4)$$

21 where $\Gamma(\cdot)$ is the Gamma function.

22 Assuming that the receiver performs the minimum mean
 23 square error (MMSE) estimation of the channel, then $\mathbf{H} =$
 24 $\hat{\mathbf{H}} + \mathbf{E}$ holds, where $\hat{\mathbf{H}}$ is the estimated channel matrix and
 25 \mathbf{E} is the estimation error. We further assume that $\hat{\mathbf{H}}$ and \mathbf{E}
 26 are uncorrelated. The entries of \mathbf{E} are also i.i.d. zero-mean
 27 circularly symmetric complex Gaussian distributed random
 28 variables with variance $\sigma_e^2 = E(h_{ij}^2) - E(\hat{h}_{ij}^2)$. The estimated
 29 SNR $\hat{\gamma}$ has the following relationship with the instantaneous
 30 SNR γ [10]

$$\hat{\gamma} = \frac{1 - \sigma_e^2}{1 + \sigma_e^2 P_T} \gamma. \quad (5)$$

32 Consequently, we can derive the PDF of the estimated
 33 SNR $\hat{\gamma}$ [9]

$$p_{\hat{\gamma}}(\hat{\gamma}) = \frac{\lambda^K}{\Gamma(K)} \hat{\gamma}^{K-1} e^{-\lambda \hat{\gamma}}, \quad \hat{\gamma} \geq 0, \quad (6)$$

35 where $\lambda = \frac{N_T R_c (1 + \sigma_e^2 P_T)}{(1 - \sigma_e^2) \bar{\gamma}}$.

The correlation between h_{ij} and its estimation \hat{h}_{ij} is [9]

$$u = \frac{E(h_{ij} \hat{h}_{ij})}{\sqrt{E(h_{ij}^2) E(\hat{h}_{ij}^2)}} = \frac{1}{\sqrt{1 + \sigma_e^2}}, \quad (7)$$

37 which indicates the quality of the channel estimation. From
 38 (5) and (7), it is clear that $\hat{\gamma} = \gamma$ and $u = 1$ hold, respec-
 39 tively, if $\sigma_e^2 = 0$. This is actually corresponding to the per-
 40 fect channel estimation. The expression (7) further tells us

41 that the correlation u between h_{ij} and \hat{h}_{ij} is getting smaller
 42 with the increase of σ_e^2 , which means that the channel esti-
 43 mation is becoming more inaccurate and will cause severe
 44 degradation of the system performance.

4. Cross-layer design in MIMO channels 47

48 The cross-layer design considered in this paper involves
 49 two layers, i.e., the physical layer and the data link layer. At
 50 the data link layer, the N_r truncated ARQ protocol is adopted.
 51 Packets received incorrectly after N_r retransmissions will
 52 be dropped, thus inducing packet loss. In order to meet the
 53 system delay constraint, for a given packet loss probability
 54 PER_{link} at the data link layer, the packet error rate (PER)
 55 P_{target} at the physical layer should be [1]

$$P_{\text{target}} = \text{PER}_{\text{link}}^{1/(N_r+1)}. \quad (8)$$

56 Since the AMC is implemented at the physical layer accord-
 57 ing to the target PER, it is clear that P_{target} is the cross-layer
 58 information.

59 Suppose that there are N MCSs at the physical layer with
 60 increasing rates R_n ($n=1, 2, \dots, N$) in terms of information
 61 bits per symbol. We will consider the modulation method
 62 with the MQAM signal constellation, where M denotes the
 63 number of points in each signal constellation. If the coding
 64 rate of a MCS is R_L , we have $R_n = R_L (\log_2 M)$. As in [1], we
 65 assume constant power transmission and adopt the equiva-
 66 lent SISO channel model to describe the estimated instan-
 67 taneous channel SNR $\hat{\gamma}$. The whole SNR range is divided
 68 into N intervals based on N thresholds γ_n , $n = 1, 2, \dots, N$.
 69 When $\gamma_n \leq \hat{\gamma} < \gamma_{n+1}$, MCS n with the rate R_n will be chosen
 70 for the next transmission. Our first task is to determine the
 71 thresholds γ_n .

72 For a fixed MCS, the relationship between the PER and
 73 $\hat{\gamma}$ can be expressed as

$$\text{PER}_n(\hat{\gamma}) = \begin{cases} 1 & \text{if } 0 < \hat{\gamma} < \gamma_{\text{cf}}, \\ f(\hat{\gamma}) & \text{if } \hat{\gamma} \geq \gamma_{\text{cf}}, \end{cases} \quad (9) \quad 75$$

76 where n is the MCS index, γ_{cf} is the SNR cut-off value
 77 indicating that no information will be transmitted when the
 78 instantaneous SNR falls below it, $f(\cdot)$ is a function obtained
 79 by a curving fitting technique according to the exact PER
 80 curve through Monte Carlo simulations. For instance, when
 81 convolutional codes act as forward error control (FEC) codes [1]

$$f(\hat{\gamma}) = a_n \exp(-g_n \hat{\gamma}), \quad (10) \quad 83$$

84 where a_n and g_n are parameters dependent on mode n . We
 85 will demonstrate in the following section that the function
 86 $f(\cdot)$ is different if we use LDPC codes as FEC codes. For a
 87 given target PER P_{target} , the thresholds can be obtained by
 88 inverting the PER expression in (9), i.e.,

$$\gamma_n = f^{-1}(P_{\text{target}}), \quad n = 1, 2, \dots, N. \quad (11) \quad 89$$

1 According to the AMC rule, each MCS n will be chosen
with the following probability [1]

$$3 \quad p_n = \int_{\gamma_n}^{\gamma_{n+1}} p_{\hat{\gamma}}(\hat{\gamma}) d\hat{\gamma} = \frac{\Gamma(K, \lambda\gamma_n) - \Gamma(K, \lambda\gamma_{n+1})}{\Gamma(K)}. \quad (12)$$

5 It can be shown that the average PER for MCS n is given
by [1]

$$\overline{\text{PER}}_n = \int_{\gamma_n}^{\gamma_{n+1}} \text{PER}_n(\hat{\gamma}) p_{\hat{\gamma}}(\hat{\gamma}) d\hat{\gamma}. \quad (13)$$

7 Then, the total average PER can be written as follows [1]:

$$\overline{P} = \frac{\sum_{n=1}^N R_n \overline{\text{PER}}_n}{\sum_{n=1}^N R_n p_n}. \quad (14)$$

9 For the ARQ with N_r retransmissions, the average number
of transmissions per packet can be expressed in terms of the
11 total average PER and N_r [1]

$$\overline{N} = \frac{1 - \overline{P}^{N_r+1}}{1 - \overline{P}}. \quad (15)$$

13 Consequently, the average spectral efficiency of the whole
system is given by [1]

$$15 \quad \overline{S}_e = \frac{\sum_{n=1}^N R_n p_n}{\overline{N}}. \quad (16)$$

5. RC-LDPC codes

17 LDPC codes are block codes that exhibit near Shannon
limit performance. They were first introduced by Gallager
19 in his thesis in 1960s [4] and rediscovered by Mackay [11]
after the debut of Turbo codes. RC-LDPC codes are a family
21 of nested codes with wide range code rates generated by a

low-rate LDPC code, which is the so-called mother code. A
lot of work has been done to find the optimum puncturing
25 and extending pattern [6], but random puncturing has been
adopted in most applications [5]. The problem of random
27 puncturing is that the receiver cannot get the puncturing pat-
tern easily. Therefore, it is difficult to put random punctur-
ing into practice. Here, we proposed a simple puncturing
29 method that is easy to implement and can get as good per-
formance as random puncturing. 31

We construct the mother code by using the progressive
edge growth (PEG) method, which has been proven to be
33 able to produce the best LDPC codes with moderate code
length and can generate a weight-increasing parity-check
35 (WIPC) matrix [12]. We employ LDPC codes with rate 1/2
(1008, 504) in our simulations. 37

The variable node degree distribution of irregular LDPC
codes is as follows: 39

$$\begin{aligned} \lambda(x) &= \sum_i \lambda_i x^i \\ &= 0.47532x^2 + 0.27953x^3 + 0.03486x^4 \\ &\quad + 0.10889x^5 + 0.10138x^{15}. \end{aligned} \quad (17)$$

Then, the bits with degree 2 are all located in the right of
the parity check matrix, corresponding to the parity check
43 bits. When constructing RC-LDPC codes, puncturing those
bits with lower degree can have less impact on the configu-
45 ration of the mother code. So, for a given rate, we implement
a continuous puncturing from those bits with the lowest de-
47 gree.

Fig. 2 gives the bit error rate (BER) performance compar-
49 ison of RC-LDPC codes with different coding rates gener-
ated by the proposed continuous puncturing and random
51 puncturing. It is clear that compared with random punctur-
ing, the proposed continuous puncturing results in similar
53 or even better performance of RC-LDPC codes. But it is

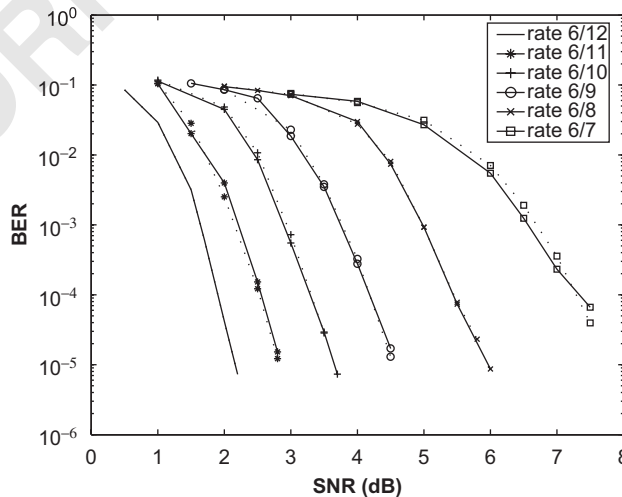


Fig. 2. BER performance comparison of RC-LDPC codes with the continuous puncturing and random puncturing (solid line: continuous puncturing; dashed line: random puncturing).

Table 1. Parameters of MCSs at the physical layer

	MCS1	MCS2	MCS3	MCS4	MCS5	MCS6
Modulation	BPSK	QPSK	QPSK	16 QAM	16 QAM	64 QAM
Coding rate	1/2	1/2	3/4	9/16	3/4	3/4
R_n (bits/sym)	0.50	1.00	1.50	2.25	3.00	4.50
a_n	2.0711	2.4654	1.3988	1.5948	1.2032	1.2086
b_n	-1.9453	1.1845	4.3105	7.2495	10.334	15.551
c_n	3.9263	3.0263	2.9004	3.4256	3.0533	2.6082
γ_{cf} (dB)	-3.3017	-0.63305	2.61	5.7713	8.7682	13.716

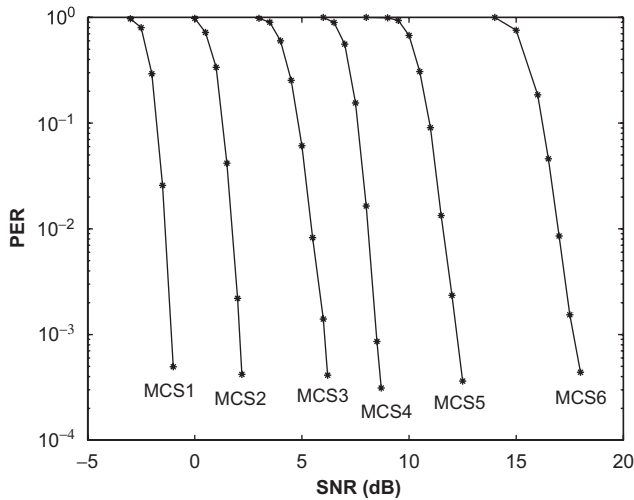


Fig. 3. PER simulation performance and fitting curves of six MCSs (star: simulation; solid line: fitting curve).

1 advantageous to use continuous puncturing with respect
 2 to the implementation of the system hardware. In the
 3 AMC-ARQ system, RC-LDPC codes constructed by con-
 4 tinuous puncturing are employed. For LDPC codes, the
 5 relationship between the PER and $\hat{\gamma}$ is given by [13]

$$PER_n(\hat{\gamma}) = \begin{cases} 1 & \text{if } 0 < \hat{\gamma} < \gamma_{cf} \\ \left(\frac{1}{1 + \exp\{c_n(\hat{\gamma} - b_n)\}} \right)^{a_n} & \text{if } \hat{\gamma} \geq \gamma_{cf} \end{cases}, \quad (18)$$

7 where a_n , b_n , c_n and γ_{cf} are parameters obtained by fitting
 (18) to the simulation results. Considering the LDPC-coded
 9 modulation schemes listed in Table 1, Fig. 3 impressively
 10 shows the excellent accordance between the theoretical ap-
 11 proximation (18) and the exact PER.

12 If we employ LDPC codes in the cross-layer design men-
 13 tioned in Section 4, the thresholds can be obtained from (11)
 and (18) as follows:

$$\gamma_n = \frac{\ln\{(1/P_{\text{target}})^{1/a_n} - 1\}}{c_n} + b_n, \quad n = 1, 2, \dots, N, \quad (19)$$

15 $\gamma_{N+1} = +\infty.$

6. Numerical results

17 In this section, numerical results showing the effects of
 18 different parameters on the spectral efficiency of our cross-
 19 layer design framework are provided. At the physical layer,
 20 the MCSs were chosen from Table 1, where the modula-
 21 tion schemes and coding rates are adopted from the IEEE
 22 802.11a standard [14]. Here, we use RC-LDPC codes in-
 23 stead of convolutional codes. Rate 3/4 and rate 9/16 LDPC
 24 codes were obtained from the rate 1/2 mother code through
 25 continuous puncturing.

26 Assume that the performance constraint at the data link
 27 layer is $PER_{\text{link}} = 0.01$. Let us consider three values for
 28 the maximum numbers of retransmissions, i.e., $N_r = 0, 1, 2$.
 29 We can get the value of P_{target} from (8). Then, the thresh-
 30 olds can be obtained from (19) and the results are shown in
 31 Table 2. When $\hat{\gamma} < \gamma_1$, which means that the channel is in
 32 deep fading and no payload bits will be sent.

33 In Fig. 4, the average spectral efficiency of the AMC-ARQ
 34 system based on RC-LDPC codes is plotted as a function
 35 of the average SNR for different values of N_r varying from
 36 0 to 2, assuming the perfect channel estimation. Curves in
 37 Fig. 4(b) denote the average spectral efficiency of the system
 38 equipped with two transmit antennas and two receive an-
 39 tennas. For comparison purposes, in Fig. 4(a) we have also
 40 plotted the performance curves for the SISO system without
 41 the STBC. The average spectral efficiency gain offered by a
 42 MIMO system over a SISO system can be remarkable. By
 43 comparing Figs. 4(a) and (b), we conclude that compared
 44 with the SISO scenario, the MIMO system employing the
 45 STBC with 2 transmit antennas and 2 receive antennas can
 46 provide at least additional 0.5 bits/symbol spectral efficiency
 47 gain for the same average SNR and an additional 4 dB diver-
 48 sity gain for the same spectral efficiency. For both SISO and
 49 MIMO scenarios, the spectral efficiency improves with the
 50 increasing N_r . The spectral efficiency gain of the AMC-ARQ
 51 system with only one retransmission ($N_r = 1$) exceeds that
 52 of the AMC-only system ($N_r = 0$) by about 0.15 bits/symbol.
 53 However, the improvement degrades quickly with the in-
 54 creasing N_r , which implies that the maximum number of
 55 retransmissions need not to be very large. A small number
 56 of retransmissions can achieve sufficient spectral efficiency
 57 gain. If we use longer LDPC codes in the AMC-ARQ sys-

Table 2. Thresholds γ_n (dB) for $N_r = 0, 1, 2$

N_r	γ_1	γ_2	γ_3	γ_4	γ_5	γ_6	γ_6
0	-1.4082	1.7463	5.4325	8.0757	11.58	17.003	∞
1	-1.7638	1.3282	4.8042	7.5924	10.908	16.22	∞
2	-1.9214	1.1361	4.5489	7.39	10.645	15.912	∞

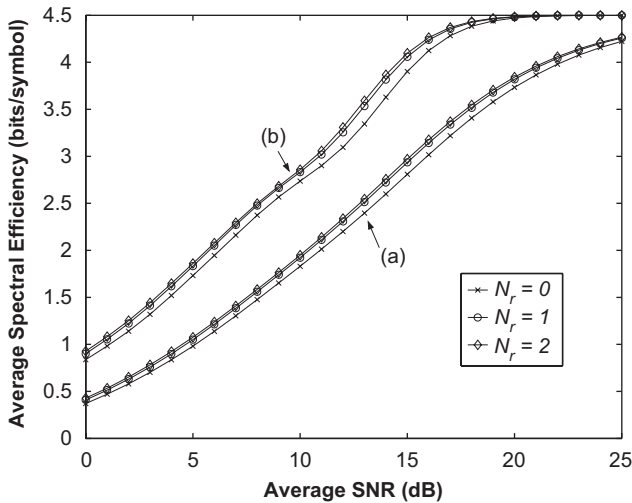


Fig. 4. Average spectral efficiency versus the average SNR for different retransmission numbers with the perfect channel estimation (a) $N_T = 1, N_R = 1$ (b) $N_T = 2, N_R = 2$.

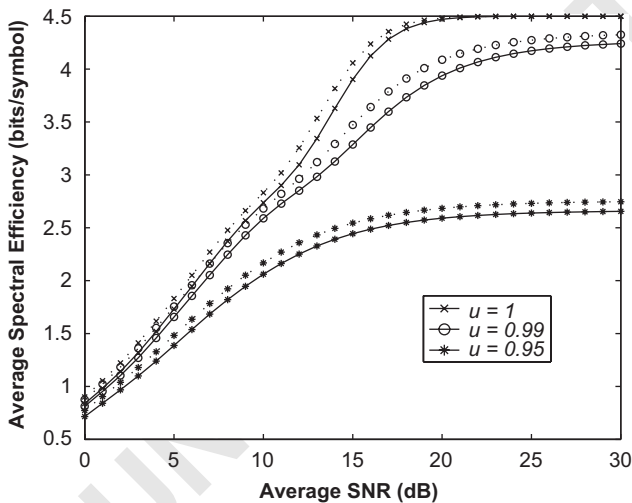


Fig. 5. Average spectral efficiency versus the average SNR for different u (dashed line: $N_r = 1$; solid line: $N_r = 0$; $N_T = 2, N_R = 2$).

is apparent that the largest average spectral efficiency can be achieved with the perfect channel estimation, i.e., $u = 1$. With the decrease of u , the average spectral efficiency is getting smaller. As we have mentioned previously, the performance of the whole system depends to a large extent on the accuracy of the channel estimation.

7. Conclusions

In this paper, we have proposed a continuous puncturing pattern for constructing RC-LDPC codes. The basic idea behind the continuous puncturing is that puncturing bits from the lowest degree will have the least impact on the mother code. Compared to the random puncturing, the proposed continuous puncturing is easier to implement and can generate similarly good RC-LDPC codes. We have applied RC-LDPC codes to the cross-layer design combining the AMC at the physical layer and the ARQ at the data link layer under MIMO fading channels using the STBC. The relevant MCS is chosen based on the SNR thresholds calculated according to the LDPC PER-SNR relationship. Furthermore, the impacts of the inaccurate channel estimation on the system spectral efficiency have also been investigated. Numerical results show that our AMC-ARQ system based on RC-LDPC codes can provide better spectral efficiency than the AMC-only system. More spectral efficiency gain can be obtained when longer LDPC codes are used.

Acknowledgements

The authors would like to acknowledge the support of the following foundations: National Scientific Foundation of China (No. 60672036) and Key Project of Provincial Scientific Foundation of Shandong (No. Z2006G04).

References

[1] Liu Q, Zhou S, Giannakis GB. Cross-layer combining of adaptive modulation and coding with truncated arq over wireless links. *IEEE Trans Wireless Commun* 2004;3: 1746–55.

[2] Hagenauer J. Rate-compatible punctured convolutional codes (rcpc codes) and their applications. *IEEE Trans Commun* 1988;36:389–400.

1 tem, the performance for the individual MCS will be better and we can get more spectral efficiency gain.

3 Fig. 5 illustrates the average spectral efficiency of the system considering different channel estimation qualities. It

- [3] Rowitch DN, Milstein LB. On the performance of hybrid fec/arq systems using rate compatible punctured turbo (rcpt) codes. *IEEE Trans Commun* 2000;48:948–59.
- [4] Li J, Narayanan K. Rate-compatible low-density parity check codes for capacity approaching arq scheme in packet data communications. In: *Proceeding of international conference on communications, internet and information technology (CIIT)*, 2002. p. 201–6.
- [5] Sesia S, Caire G, Vivier G. Incremental redundancy hybrid arq schemes based on low-density parity-check codes. *IEEE Trans Commun* 2004;52:1311–21.
- [6] Yazdani MR, Banihashemi AH. On construction of rate-compatible low-density parity-check codes. *IEEE Commun Lett* 2004;8:159–61.
- [7] Tarokh V, Jafarkhani H, Calderbank AR. Space-time block codes from orthogonal designs. *IEEE Trans Inf Theory* 1999;45:1456–67.
- [8] Ganesan G, Stoica P. Space-time block codes: a maximum snr approach. *IEEE Trans Inf Theory* 2001;47:1650–6.
- [9] Lu D. *Stochastic process and its application*. Beijing, China: Tsinghua University Press; 1986.
- [10] Baltersee J, Fock G, Meyr H. Achievable rate of mimo channels with data-aided channel estimation and perfect interleaving. *IEEE J Selected Areas Commun* 2001;19: 2358–68.
- [11] MacKay DJC, Neal RM. Near shannon limit performance of low density parity check codes. *Electron Lett* 1996;32: 1645–6.
- [12] Hu X, Eleftheriou E, Arnold DM. Regular and irregular progressive edge growth tanner graphs. *IEEE Trans Info Theory* 2005;51:386–98.
- [13] MacKay DJC, Hesketh CP. Performance of low density parity check codes as a function of actual and assumed noise levels. *Electronic notes in theoretical computer science*, 2003.
- [14] Doufexi A, Armour S, Butler M, Nix A, Bull D, McGeehan J, Karlsson P. A comparison of the hiperlan/2 and ieee 802.11a wireless lan standards. *IEEE Commun Mag* 2002;40: 172–80.



Yuling Zhang received her B.E. and Ph.D. degrees in communication and information systems from Shandong University, Shandong, PR China, in June 2002 and June 2007, respectively. Now she is a lecturer in the School of Computer Science and Technology at Ludong University, Shandong, PR China. Till now, she has published more than ten papers in journals and conference proceedings. Her current research interests include LDPC codes and cross-layer design.



Dongfeng Yuan received his M.S. degree from Department of Electrical Engineering, Shandong University, China, 1988, and got his Ph.D. degree from Department of Electrical Engineering, Tsinghua University, China in January 2000. Currently, he is a full professor and dean in School of Information Science and Engineering, Shandong University, China. He is a senior

member of IEEE and a senior member of China Institute of Communications and China Institute of Electronics.

From 1993 to 1994, he was a visiting professor in the Electrical and Computer Department at the University of Calgary, Alberta, Canada, a visiting professor in Department of Electrical Engineering in the University of Erlangen, Germany, 1998–1999, a visiting professor in Department of Electrical Engineering and Computer Science in the University of Michigan, Ann Arbor, USA, 2001–2002. He has published over 200 papers in technical journals and at international conferences in his research field recently. His research interests include: Multilevel Coding and Multistage Decoding, Space-Time Coded Modulation, Turbo Codes, LDPC codes, Cross-layer design, Multicarrier modulation for high speed transmission in 4G and Unequal Error Protection characteristics in multimedia transmission in fading channels.



Cheng-Xiang Wang received the B.Sc. and M.E. degrees in communication and information systems from Shandong University, PR China, in 1997 and 2000, respectively, and the Ph.D. degree in wireless communications from Aalborg University, Denmark, in 2004. From 2000 to 2001, Dr. Wang was a Research Assistant with Technical University of Hamburg-Harburg, Germany.

From 2001 to 2005, he was a Research Fellow with Agder University College, Norway. From January to April 2004, he was a Visiting Researcher at Siemens AG-Mobile Phones, Munich, Germany. Since 2005, he has been a lecturer at Heriot-Watt University, Edinburgh, UK. He is also an honorary fellow of the University of Edinburgh, a guest researcher of Xidian University, and an adjunct professor of Guilin University of Electronic Technology, PR China. His current research interests include mobile propagation channel modeling, MIMO, OFDM, UWB, cognitive radio, cooperative communications, and cross-layer design of wireless networks. He has published about 80 papers in journals and conferences.

Dr. Wang serves as an Editor for *Wireless Communications and Mobile Computing (WCMC) Journal*, *Security and Communication Networks Journal*, and *Journal of Computer Systems, Networks, and Communications*. He is a TPC member for 16 international conferences including IEEE Globecom 2006, ICC 2007, and ICC 2008.